

## Effect of pore size on effective conductivity of UO<sub>2</sub>: A computational approach

Bohyun Yoon, Kunok Chang \*

Department of Nuclear Engineering, Kyung Hee University, Yong-in city, Korea

\*Corresponding author: kunok.chang@khu.ac.kr

### 1. Introduction

The thermal conducting properties of UO<sub>2</sub> pallet degrade over lifetime of a nuclear power plant and it can be a critical limiting factor of the safety and efficiency of the reactor [1-3]. A commercial UO<sub>2</sub> pallet contains microstructural inhomogeneities, such as grain boundaries, voids and He/Xeon bubbles [4-15]. Since those microstructural defects seriously affect thermal conductivity of the nuclear fuel, understanding correlation between effective thermal conductivity and temporal distribution of the imperfections is a quite important task. For decades, the prediction of effective conductivity of porous nuclear fuel largely depend on Maxwell-Eucken (hereafter ME) model [8] which is adopted in FRAPCON [16]. Including ME model, the effective thermal conductivity models of nuclear fuel do not reflect the effect of pore size [4-15]. There have been an widely accepted assumption that the pore size is much larger than the average phonon wavelength [4], therefore, the effect of pore size on the effective thermal conductivity has not been of much concern for decades. However, whether the assumption in the previous sentence is valid has not been thoroughly examined in an experimental study or continuum modeling. We investigated a role of pore size by means of the continuum-level simulations. We performed the steady-state heat conduction analysis in 2-D and 3-D systems and the effect of the pore size on the effective conductivity was evaluated systematically.

### 2. Methods and Results

#### 2.1 Microstructure and temperature dependence on local conductivity

We introduced the non-conserved structural order parameter  $\eta_i(r)$  which the value is 0 in the He bubble region and 1 at the matrix [10]. Within an interfacial region, its parameter value diffuses smoothly. The thermal conductivity of He gas is fixed at 0.152 W/(K·m), and the conductivity of UO<sub>2</sub> crystal is taken from the model suggested by Harding and Martin which has the following temperature dependence in the unit of W/(K·m) [17].

$$k_{crystal} = \frac{1}{0.0375 + 2.165 \times 10^{-4} T} + \frac{4.715 \times 10^9}{T^2} \exp\left(\frac{-16361}{T}\right) \dots (1)$$

The effect of structural order parameter  $\eta_i(r)$  on the local heat conductivity is

$$k(r) = \sum_i \eta_i^6(r) \times k_{crystal} \dots (2)$$

Miller et al. proposed effective conductivity model of polycrystalline UO<sub>2</sub> with pores as follows: [9]

$$k_{eff} = \frac{k_0}{1 + k_0/G_k d} (1 - P)^\beta \Psi \dots (3)$$

where  $G_k$  is a Kapitza conductance,  $d$  is an average grain diameter,  $\beta$  is a fitting parameter and  $\Psi=1-P$  is a correlation factor that relates 2-D to 3-D heat transport in porous media (for  $P < 10.0\%$ ).

In their model, they incorporated phonon scattering at the grain boundary, therefore, they assumed that the effective heat conductivity at the grain boundary is lower than the value in the matrix [9].

In Eq. 4, so called ‘‘Schulz equation’’ [18],  $\beta$  is determined by geometry of pores.

Nikolopoulos and Ondracek proposed the model for effective conductivity of porous material ( $k_{eff}$ ) at given porosity ( $P$ ) with conductivity of nonporous material ( $k_0$ ) [14].

$$k_{eff} = k_0 (1 - P)^\beta \dots (4)$$

Nikolopoulos and Ondracek predicted  $\beta=2.5$  for spherical pores and  $\beta=1.667$  for cylindrical pores which statistically directed to the field direction in isotropic materials [14].

#### 2.2 Steady-state thermal conduction analysis

We solved steady-state heat conduction equation as follows:

$$\nabla k(r) \nabla T(r) = 0 \dots (5)$$

In 2-D, we simulated 10.24  $\mu\text{m}$  ( $L_x$ )  $\times$  10.24  $\mu\text{m}$  ( $L_y$ ) system. The simulation cell size is 1024 $\times$ 1024 grid points, therefore  $\Delta x = \Delta y = 10$  nm. For boundary conditions, Dirichlet boundary condition of  $T=800\text{K}$  is applied on the line of  $x=0$  and Neumann boundary condition of  $j = k(r) \frac{\partial T(r)}{\partial x} = 50\text{MW}/\text{m}^2$ , constant heat flux condition is applied across the line  $x=10.24 \mu\text{m}$ . We applied the adiabatic condition,  $\frac{\partial T(r)}{\partial x} = 0$  when  $y=0, 10.24 \mu\text{m}$ . The effective thermal conductivity is evaluated by the relation [12]:

$$k_{eff} = \frac{j \times L_x}{\Delta T} \dots (6)$$

where  $j$  is the heat flux.

To calculate  $\Delta T$ , we evaluate the average temperature of the line,  $x=0$  and  $x=L_x$  and find the difference of them.

#### 2.3 Crank-Nicolson method

We solve steady-state heat conduction equation using a finite-difference approximation based on the Crank-Nicolson scheme (CN) and alternating-direction-implicit (ADI) method. The CN scheme is an implicit method

which discretizes time and space. And we apply Douglas-Gunn's ADI splitting method to decompose the discretization matrix of the CN scheme. This ADI method splits the matrix into three simple matrices introducing intermediate time steps between  $n$  and  $n+1$ .

With the notations  $\delta^2$  and  $\delta$  defined as:

$$\delta_x^2 u(r) = u(r)_{i-1,j,k} - 2u(r)_{i,j,k} + u(r)_{i+1,j,k} \dots (7)$$

$$\delta_x u(r) = u(r)_{i+1,j,k} - u(r)_{i-1,j,k} \dots (8)$$

And letting  $C$  as:

$$C_x = \frac{D(u)\Delta t}{(\Delta x)^2} \delta_x^2 + \left( \frac{\delta_x D(u)\Delta t}{4(\Delta x)^2} \right) \delta_x \dots (9)$$

The CN method applied steady-state heat conduction equation can be arranged to:

$$\left[ 1 - \frac{C_x}{2} - \frac{C_y}{2} - \frac{C_z}{2} \right] u(r)^{n+1} = \left[ 1 + \frac{C_x}{2} + \frac{C_y}{2} + \frac{C_z}{2} \right] u(r)^n \dots (10)$$

This equation can be factorized and using a Douglas-Gunn method:

$$\left( 1 - \frac{C_x}{2} \right) u(r)^{n+\frac{1}{3}} = \left( 1 + \frac{C_x}{2} + C_y + C_z \right) u(r)^n$$

$$\left( 1 - \frac{C_y}{2} \right) u(r)^{n+\frac{2}{3}} = \left( 1 + \frac{C_x}{2} + \frac{C_y}{2} + C_z \right) u(r)^n + \frac{C_x}{2} u(r)^{n+\frac{1}{3}}$$

$$\left( 1 - \frac{C_z}{2} \right) u(r)^{n+1} = \left( 1 + \frac{C_x}{2} + \frac{C_y}{2} + \frac{C_z}{2} \right) u(r)^n + \frac{C_x}{2} u(r)^{n+\frac{1}{3}} + \frac{C_y}{2} u(r)^{n+\frac{2}{3}} \dots (11)$$

#### 2.4 Porous material with different pore sizes

According to our best knowledge, the effect of porosity and temperature on the effective conductivity of  $UO_2$  has been studied in depth, while the effect of pore size has not been studied. [5-15]

To examine the pore size effect on effective conductivity in 2D and 3D, we measured effective conductivity with different pore sizes. In 2D, we examined 8 different pore sizes, which is homogeneous in the system. The system size is  $2048\Delta x \times 2048\Delta y$  ( $10.24 \mu m \times 10.24 \mu m$ ).

We introduced the structural order parameter  $\phi$  which value is 1.0 in non-porous region and 0.0 in porous region. The parameter varies smoothly at the interface region to enhance the numerical stability of the effective conductivity calculation. We found that the exponent  $\beta$  in Eq. 4 increases as the pore size decreases, which means small pore-sized structure has stronger dependency of porosity in effective conductivity rather than large pore-sized structure.

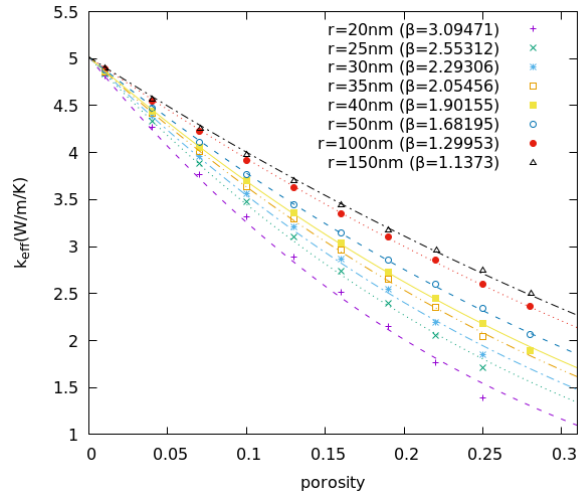


Fig. 1. Effective conductivity ( $k_{eff}$  with function of porosity) at different pore sizes in 2D.

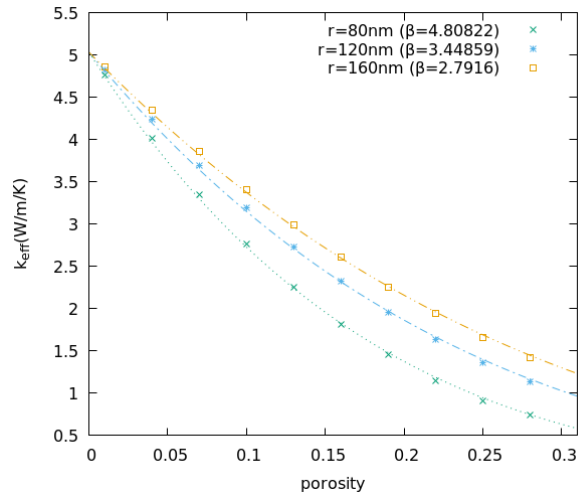


Fig. 2. Effective conductivity ( $k_{eff}$  with function of porosity) at different pore sizes in 3D.

### 3. Conclusions

In this work, we have investigated a role of pore size on effective conductivity of  $UO_2$  using the computational method in 2D and 3D systems at continuum-level. The calculations reveal that small pores are more effective in reducing effective conductivity rather than large pores at given porosity in both 2D and 3D systems. We found the exponent value  $\beta$  of Schulz equation and we found that there is a dependence of pore size on exponent  $\beta$  value. We assumed all pore size is same in the system and we found that  $\beta$  exponent decreases as the pore size increases in 2D and 3D.

### REFERENCES

- [1] P. Lucuta, H. Matzke, I. Hastings, A pragmatic approach to modeling thermal conductivity of irradiated  $UO_2$  fuel: review and recommendations, Journal of nuclear materials 232 (2-3) 166-180 (1996).

- [2] H. R. Trellue, Safety and neutronics: A comparison of  $\text{MOX}$  vs  $\text{UO}_2$  fuel, *Progress in Nuclear Energy* 48 (2) 135-145 (2006).
- [3] R. Ohse, P. Berrie, H. Bogensberger, E. Fischer, Extension of vapour pressure measurements of nuclear fuels ( $\text{U}$ ,  $\text{Pu}$ )  $\text{O}_2$  and  $\text{UO}_2$  to 7000 K for fast reactor safety analysis, *Journal of Nuclear Materials* 59 (2) 112-124 (1976).
- [4] S. R. Phillpot, A. El-Azab, A. Chernatynskiy, J. S. Tulenko, Thermal conductivity of  $\text{UO}_2$  fuel: Predicting fuel performance from simulation, *JOM* 63 (8) 73 (2011).
- [5] C.-W. Lee, A. Chernatynskiy, P. Shukla, R. E. Stoller, S. B. Sinnott, S. R. Phillpot, Effect of pores and He bubbles on the thermal transport properties of  $\text{UO}_2$  by molecular dynamics simulation, *Journal of Nuclear Materials* 456 253-259 (2015).
- [6] X.-M. Bai, M. R. Tonks, Y. Zhang, J. D. Hales, Multiscale modeling of thermal conductivity of high burnup structures in  $\text{UO}_2$  fuels, *Journal of Nuclear Materials* 470 208-215 (2016).
- [7] M. R. Tonks, X.-Y. Liu, D. Andersson, D. Perez, A. Chernatynskiy, G. Pastore, C. R. Stanek, R. Williamson, Development of a multiscale thermal conductivity model for fission gas in  $\text{UO}_2$ , *Journal of Nuclear Materials* 46 (3) 253-258 (1973).
- [8] G. Ondracek, B. Schulz, The porosity dependence of the thermal conductivity for nuclear fuels, *Journal of Nuclear Materials* 46 (3) 253-258 (1973).
- [9] P. C. Millett, D. Wolf, T. Desai, S. Rokkam, A. El-Azab, Phase-field simulation of thermal conductivity in porous polycrystalline microstructures, *Journal of Applied Physics* 104 (3) 033512 (2008).
- [10] P. C. Millett, M. Tonks, Meso-scale modeling of the influence of intergranular gas bubbles on effective thermal conductivity, *Journal of Nuclear Materials* 412 (3) 281-286 (2011).
- [11] K. Chockalingam, P. C. Millett, M. Tonks Effect of intergranular gas bubbles on thermal conductivity, *Journal of Nuclear Materials* 430 (1-3) 166-170 (2012).
- [12] P. C. Millett, M. R. Tonks, K. Chockalingam, Y. Zhang, S. Biner, Three dimensional calculations of the effective Kapitza resistance of  $\text{UO}_2$  grain boundaries containing intergranular bubbles, *Journal of Nuclear Materials* 439 (1-3) 117-122 (2013).
- [13] P. Nikolopoulos, S. Nazare, F. Thummler, Surface, grain boundary and interfacial energies in  $\text{UO}_2$  and  $\text{UO}_2\text{-Ni}$ , *Journal of Nuclear Materials* 71 (1) 89-94 (1977).
- [14] P. Nikolopoulos, G. Ondracek, Conductivity bounds for porous nuclear fuels, *Journal of Nuclear Materials* 114 (2-3) 231-233 (1983).
- [15] P. Sens, The kinetics of pore movement in  $\text{UO}_2$  fuel rods, *Journal of nuclear materials* 43 (3) 293-307 (1972).
- [16] K. Geelhood, W. Luscher, Frapcon-4.0: integral assessment, Pacific Northwest National Laboratory, PNNL-19418 2 (2015).
- [17] J. Harding, D. Martin, A recommendation for the thermal conductivity of  $\text{UO}_2$ , *Journal of nuclear materials* 166 (3) 223-226 (1989).
- [18] B. Schulz, Thermal conductivity of porous and highly porous materials, *High Temperatures-High Pressures* 13 (6) 649-660 (1981).